Available online at www.sciencedirect.com
SCIENCE DIRECT®
Journal of Catalysis 229 (2005) 344–351
JOURNAL OF CATALYSIS
www.elsevier.com/locate/jcat

Reaction of nanocrystalline MgO with 1-iodobutane

Ilya V. Mishakov [a], David S. Heroux [b], Vladimir V. Chesnokov [a], Sergey G. Koscheev [a], Maxim S. Mel'gunov [a], Alexander F. Bedilo [a], Roman A. Buyanov [a], Kenneth J. Klabunde [b,*]

[a] *Boreskov Institute of Catalysis, Novosibirsk 630090, Russia*
[b] *Department of Chemistry, Kansas State University, Manhattan, KS 66506, USA*

Received 20 February 2003; revised 29 March 2004; accepted 28 October 2004

Available online 23 December 2004

Abstract

The dehydroiodination of 1-iodobutane has been investigated over two different nanocrystalline MgO samples. The reaction with clean MgO takes place at temperatures as low as 100 °C. However, a temperature of 300 °C or higher is required for catalytic dehydroiodination to take place. At lower temperatures the reaction stops after the maximum degree of surface modification with iodine is reached. It was found by XPS that at all temperatures iodination is limited to the surface and no bulk MgI_2 is formed. The weight gain never exceeds 22%, which corresponds to 3.7% MgO conversion. In accordance with this conclusion, the textures of the samples after reaction are similar to those of the initial MgO. The surface iodination leads to a change in reaction mechanism: from concerted E2 elimination on initial MgO to stage E1 elimination. The secondary process of 2-iodobutane formation over iodinated samples was also established.

1. Introduction

Nanocrystalline alkaline earth metal oxides attract significant attention as effective chemisorbents for such toxic gases as NO_2, SO_2, SO_3, and HCl and chlorinated and phosphorous-containing compounds [1–9]. For example, it has been shown that CCl_4 reacts with nanocrystalline aerogel-prepared MgO (AP-MgO) at 500 °C according to reaction (1).

$$2MgO + CCl_4 \rightarrow 2MgCl_2 + CO_2. \quad (1)$$

We recently studied in detail the destructive adsorption of several chlorobutanes over AP-MgO at 50–400 °C [10,11]. It has been found that the chlorobutanes are subjected to selective dehydrochlorination with HCl abstraction and formation of a mixture of butene isomers. Hydrogen chloride formed in this process reacted with nanocrystalline MgO to yield a new phase of $MgCl_2$. Another important feature of 1-chlorobutane dehydrochlorination over AP-MgO is the significant changes in the texture of the material. It was found that a 50–70% MgO transformation into $MgCl_2$ leads to a drop in the surface area from about 400 m^2/g to 20–40 m^2/g, so that the pores present in the initial oxide are mostly filled with magnesium chloride. Still, despite this more than 10-fold drop in the surface area, the formation of $MgCl_2$ results in a 5-fold increase in the catalytic activity. Similar tendencies were observed for dehydrobromination of 1-bromobutane as well [10].

In addition, nanocrystalline MgO itself and MgO modified with vanadium oxide were found to be efficient catalysts in one-step selective oxidative dehydrogenation of butane to butadiene in the presence of oxygen and iodine [12]. Molecular iodine shifts the equilibrium of the dehydrogenation reactions toward reaction products and makes it possible to achieve high butane conversion with high selectivity for butadiene. However, the iodine addition to the feed leads to the formation of iodinated organic compounds, including 1-iodobutane. The concentration of such iodinated compounds may reach 10–15 wt% of the butadiene obtained [13]. This problem makes investigation of iodine regeneration from iodinated organic compounds very important.

* Corresponding author.
E-mail address: kenjk@ksu.edu (K.J. Klabunde).

0021-9517/$ – see front matter
doi:10.1016/j.jcat.2004.10.026

In the current publication we report on the reaction of 1-iodobutane with nanocrystalline MgO prepared by two different techniques. There are two reasons to gain an understanding of the 1-iodobutane system: (1) to establish whether general observations for chloro- and bromo-derivatives carry over to the iodo-system, leading to a better understanding of the overall reaction, and (2) to establish whether iodobutanes are likely intermediates in the dehydrogenation of butane over nanocrystalline MgO in the presence of iodine as an additive,

2. Experimental

The following nanocrystalline oxides were used in the experiments: AP-MgO (410 m^2/g) and CP-MgO (280 m^2/g). CP-MgO was obtained by decomposition of $Mg(OH)_2$ prepared by overnight hydration of commercial MgO (Aldrich) in refluxing water followed by evacuation at 500 °C. Preparation of AP-MgO has been described in detail elsewhere [14]. In short, this includes preparation of $Mg(OCH_3)_2$ via reaction of Mg with CH_3OH, dilution of $Mg(OCH_3)_2$ with toluene, formation of $Mg(OH)_2$ with water addition, supercritical drying of the $Mg(OH)_2$ suspension, and conversion of $Mg(OH)_2$ to AP-MgO via heat treating under a dynamic vacuum at 500 °C overnight.

The reaction was performed in a flow reactor equipped with a McBane spring balance, which made it possible to monitor changes in the catalyst weight during the reaction with a 10^{-4} g precision. 1-Iodobutane was introduced into the reactor by saturation of the argon flow with 1-iodobutane its vapor at room temperature to give a 2% C_4H_9I concentration in the feed. The volume flow rate was 2 l/h, and the catalyst loading was varied within 0.05–0.1 g. The product composition after the reactor was analyzed by gas chromatography. Prior to each run the samples were activated in the argon flow at 500 °C for 30 min for removal of adsorbed water.

The iodine and carbon contents were determined by elemental analysis and X-ray fluorescence spectral analysis (XFSA) on a VRA-20 analyzer with an external standard with a relative error of 10%.

XPS studies of AP-MgO after reaction with 1-iodobutane were performed with a VG ESCALAB (VG Scientific) electron spectrometer. The samples were attached to the holder with a conducting vacuum-stable two-sided sticking tape in air. Prior to the spectroscopic experiments the samples were evacuated in a pretreatment chamber down to 10^{-7} mbar. Then they were moved into the analyzer chamber with a basis vacuum better than 10^{-9} mbar. The main background gases were CO, CO_2, and H_2O.

Studies of nitrogen adsorption at 77 K were carried out with an ASAP 2400 instrument (Micromeritics). The N_2 adsorption isotherms were analyzed by the BET method and the comparative plot method [16,17] based on a comparison of the variation of adsorption uptake of experimental adsorption isotherm (EI) with a reference adsorption isotherm (RI) for a nonporous sample (generally it is analogous to a more widely used α_S method [18]). The isotherm reported in Refs. [14,15] was used as the RI.

3. Results and discussion

3.1. Gravimetric measurements

It has been found that the reaction of nanocrystalline AP-MgO with 1-iodobutane in the temperature range of 100–400 °C is accompanied by an increase in the sample weight. The kinetic graphs of the weight change presented in Fig. 1 indicate that the maximum weight gain depends on the reaction temperature. The smallest gain (4.1 wt%) was observed at 400 °C (Fig. 1, curve 5). In this case the maximum weight is achieved already after 40 min on stream and does not change after that. The maximum weight grew as the reaction temperature was decreased; the highest value of 22.5% was obtained at 200 °C (Fig. 1, curve 4).

The chromatographic analysis of the outlet gases after the reactor indicated the presence of three butene isomers. This observation brought us to the conclusion that HI is abstracted from 1-iodobutane, and its following reaction with MgO leads to the weight gain. We believe that, in this case, similar to the reactions of 1-chlorobutane and 1-bromobutane over AP-MgO that result in the formation of $MgCl_2$ and $MgBr_2$, respectively [10], the weight gain is due to the formation of MgI_2. Since the molecular weight of magnesium iodide is approximately 7 times larger than that of MgO, we could expect a 600% weight gain if the oxide were completely converted into iodide. However, the actual weight gain was just above 20%. If the MgO conversion to MgI_2 is the only

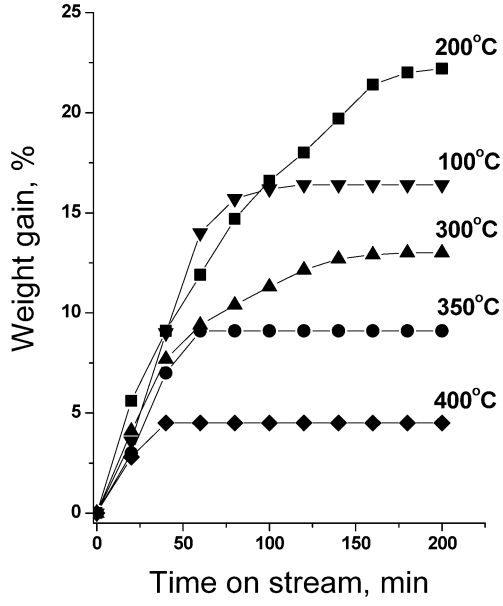

Fig. 1. Change of the sample weight during reaction of AP-MgO with 1-iodobutane at different temperatures.

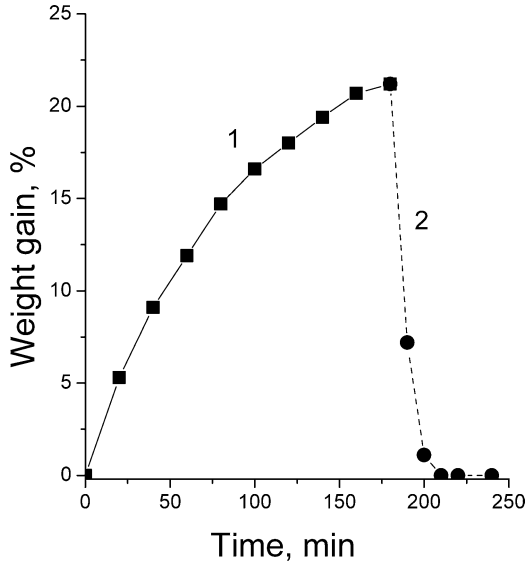

Fig. 2. Weight change of AP-MgO subjected to reaction with 1-iodobutane at 200 °C (1), and following calcination in argon flow at 500 °C (2).

cause of the weight gain, this corresponds to a 3.7% conversion. It is notable that nearly 60% conversion of MgO to $MgCl_2$ was observed during the reaction of AP-MgO with 1-chlorobutane under similar conditions [10]. This indicates that the MgO conversion to MgI_2 is mostly limited to the surface. This is due most likely to a much larger size of I^- ions in comparison with Cl^- and Br^-, which hinders iodine diffusion into the MgO lattice and substitution of the lattice oxide for iodine. This conclusion is substantiated by the XRD results. MgI_2 was not observed by XRD in any of the AP-MgO samples after reaction with 1-iodobutane. This means that after reaction iodine is present only in the form of surface compounds, and no bulk MgI_2 is formed.

Fig. 2 presents the weight changes in an AP-MgO sample first subjected to reaction with 1-iodobutane at 200 °C (curve 1) and then heat-treated in an argon flow at 500 °C (curve 2). It is clear that the calcination in argon results in the complete loss of the 22 wt% gained during the reaction with 1-iodobutane.

3.2. Activity and selectivity of MgO in dehydroiodination of 1-iodobutane

Dehydroiodination of 1-iodobutane over AP-MgO was studied in the temperature range of 100–400 °C. Fig. 3 presents experimental dependence of the 1-iodobutane conversion over AP-MgO as a function of time on stream at different temperatures. At 100 °C the percentage conversion decreases from the initial 45% to nearly zero in 3 h (Fig. 3, curve 1). The same tendency is observed at 200 °C (curve 2). In this case, the conversion gradually decreases to 4–5% in 6 h on stream. However, a temperature increase to 300 °C results in stabilization of the 1-iodobutane conversion at 69% (curve 3). Further increase in the reaction temperature leads to conversion growth to nearly 100% at 400 °C.

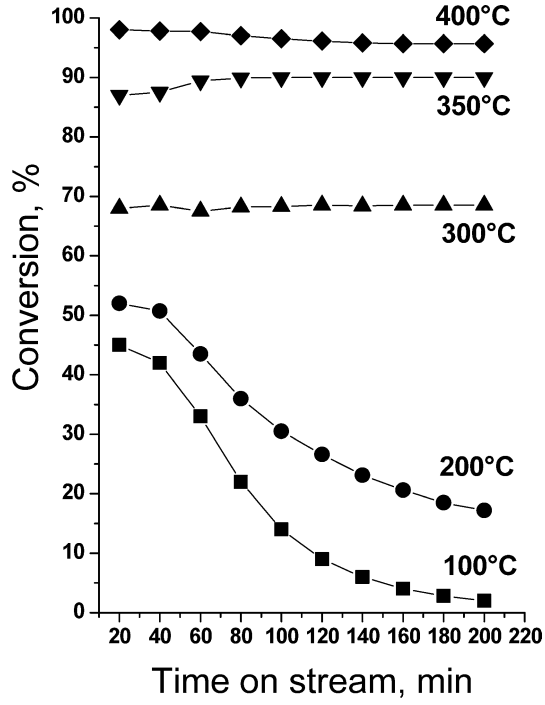

Fig. 3. Dependence of 1-iodobutane conversion over AP-MgO on time on stream at different temperatures.

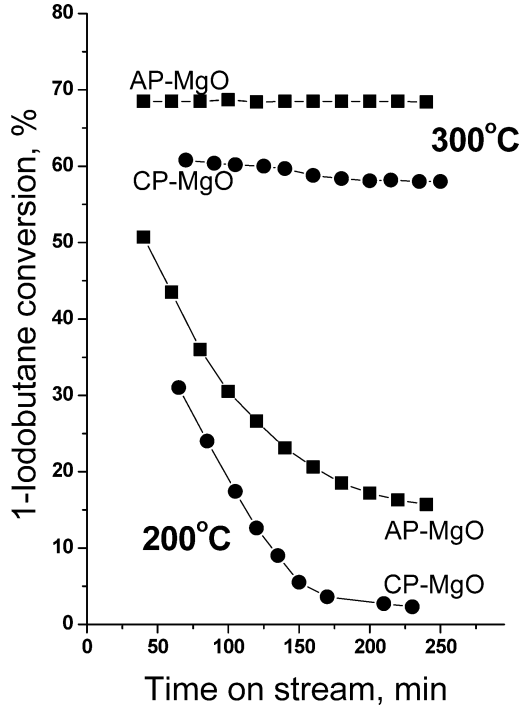

Fig. 4. 1-Iodobutane conversion over AP-MgO and CP-MgO at 200 and 300 °C.

The activities of AP-MgO and CP-MgO in dehydroiodination of 1-iodobutane are compared in Fig. 4. The graph shows that the activity of AP-MgO is higher than that of CP-MgO at any temperature studied. Furthermore, at 200 °C CP-MgO looses all of its activity in 4 h. Higher dehy-

droiodination activity of AP-MgO in comparison with CP-MgO correlates well with earlier data on destructive adsorption of various compounds [7–9,22,23]. However, reaction rates normalized to the surface areas of materials measured after reaction at 300 °C were found to be very similar: 0.113 mmol/(h m^2) for CP-MgO and 0.117 mmol/(h m^2) for AP-MgO.

As noted above, dehydroiodination of 1-iodobutane over AP-MgO yields a mixture of three butene isomers: 1-butene, *cis*-2-butene, and *trans*-2-butene. Mechanistically, in contact elimination, as in the liquid phase, it is necessary to distinguish between three main possibilities [24]. The reaction following the E1 mechanism starts with X^- abstraction, generating a carbocation, which has a certain lifetime and can be subjected to rearrangement before it loses a proton in the second step. In the case of the E1cB mechanism the reaction also consists of two distinct steps, beginning with the proton abstraction. The E2 mechanism covers a broad range between the two, with H^+ and X^- removed simultaneously in a concerted process. Its essential feature is that the energy process has only one maximum.

If no rearrangement of the carbocation takes place, which is typical for the concerted E2 reaction mechanism, 1-butene should be the only product resulting from the dehydrochlorination of 1-chlorobutane. It was important to determine whether the surface modification during the reaction resulted in any significant changes in the mechanism of the HI elimination. Earlier we observed that changes in the phase composition of the catalyst affected the distribution of the butene isomers formed during dehydrochlorination of 1-chlorobutane over AP-MgO [10]. During the first minutes of the reaction with 1-chlorobutane when the catalysts consisted mostly from the MgO phase, 1-butene was formed with nearly 100% selectivity. The formation of magnesium chloride resulted in a significant increase in the selectivity toward *cis*-2-butene and *trans*-2-butene. This observation was explained by a change in the reaction mechanism. It was suggested that the HCl abstraction over MgO follows the E2 mechanism. Meanwhile, the E1 abstraction mechanism predominates over $MgCl_2$ formed in the reaction of MgO with HCl. This mechanism involves the formation of intermediate carbocation that is subjected to fast isomerization to yield three butene isomers.

Changes in the relative selectivity for these three isomers with time on stream at 300 and 400 °C are presented in Fig. 5. At 300 °C the 1-butene selectivity at the fifth minute after the start of the reaction is nearly 100%. Within 2 h it decreases by a factor of 4 and stabilizes at 23%. Meanwhile the selectivities for *cis*-2-butene and *trans*-2-butene reach 50 and 27%, respectively, and do not change further more. A comparison of these data with the weight gain curve (Fig. 1, curve 3) led us to an obvious conclusion that these changes in the selectivity are due entirely to modification of the MgO surface in the course of reaction. During the first minutes HI abstraction from 1-iodobutane takes place on a nearly clean MgO surface and follows a concerted E2

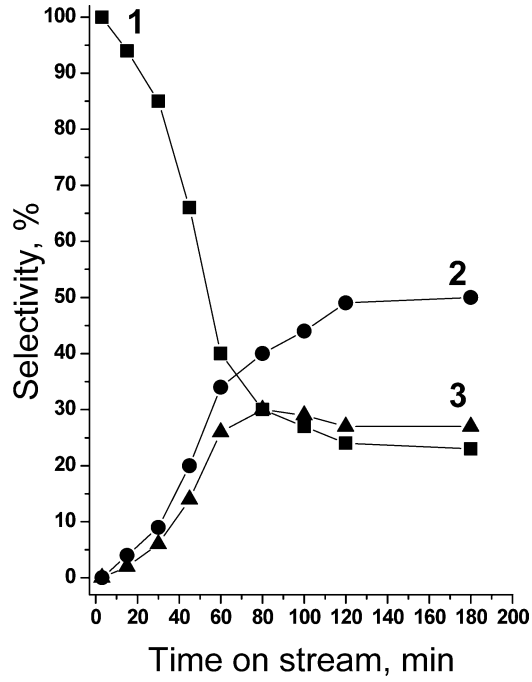

Fig. 5. Dependence of AP-MgO selectivity at 300 °C on time on stream. 1—1-butene; 2—*cis*-2-butene; 3—*trans*-2-butene.

mechanism that yields only 1-butene. Full iodination of the surface leads to predomination of the E1 reaction mechanism when all three isomers are formed in comparable amounts. Similar behavior has been observed elsewhere for dehydrochlorination of 1-chlorobutane over AP-MgO [10].

It is also notable that the amounts of *cis*-2-butene formed in the reaction are always higher than those of the trans-isomer. This observation seems to contradict the thermodynamics. However, such behavior is often observed in contact eliminations [10,24,25]. It can be attributed to natural steric limitations on the surface that hinder the formation of *trans*-2-butene.

Besides the dehydroiodination reaction, a secondary reaction of HI with butene that results in the formation of 2-iodobutane has been observed over iodinated MgO. This reaction results in a decrease in the process selectivity for butenes. Fig. 6 shows that for both MgO samples the formation of 2-iodobutane starts only after the maximum degree of iodination of the MgO surface is reached and HI no longer reacts with MgO. It is interesting that at the same temperature (300 °C) the selectivity for 2-iodobutane is higher over CP-MgO than it is over AP-MgO). This observation can be explained as follows. The atom of iodine, after abstraction on the surface magnesium atom (first step of stage E1 mechanism), can react again with carbocation to form 2-iodobutane. The lower selectivity for 2-iodobutane over AP-MgO indicates that the surface Mg–I bond in the AP sample is stronger than that in the CP sample. One can conclude that the strength of Lewis sites in AP-MgO is higher in comparison with CP-MgO. This is probably due to the unique chemistry of nanoscale magnesium oxide.

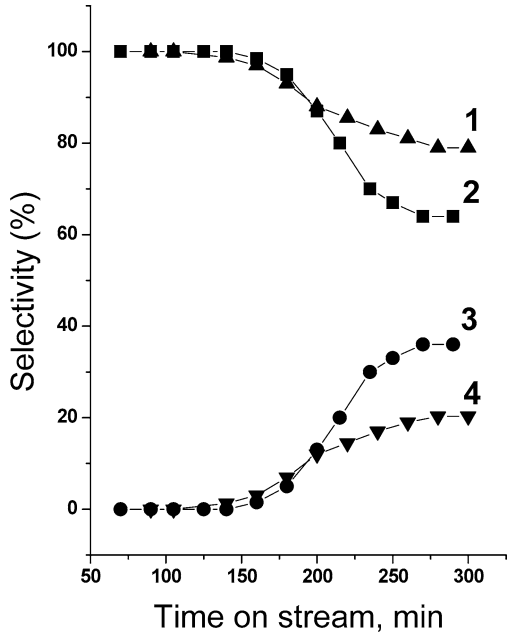

Fig. 6. Selectivity of AP-MgO (1, 4) and CP-MgO (2, 3) in dehydroiodination of 1-iodobutane at 300 °C: 1, 2—total of butene isomers; 3, 4—2-iodobutane.

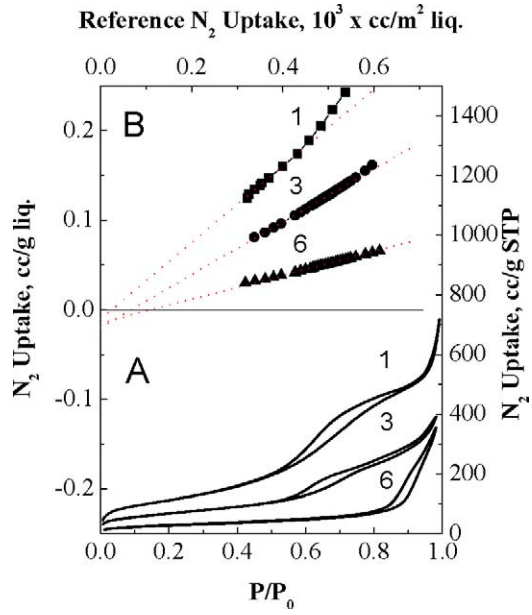

Fig. 7. N_2 adsorption isotherms in (A) regular coordinates (bottom x-axis, left y-axis), and (B) coordinates of the comparative plot method (top x-axis, right y-axis).

3.3. Thermodynamic considerations

A thermodynamic estimation of the feasibility of HI abstraction from a 1-iodobutane molecule to form 1-butene [10] indicates that considerable 1-iodobutane conversion should be expected only at temperatures above 350 °C. However, in the experiments we observed a significant conversion (above 40%) during the first minutes, even at 100 °C. Subsequent fast decrease of the activity to zero brings us to the conclusion that at this temperature the HI abstraction from 1-iodobutane is possible only because of the iodination of magnesium oxide.

$$C_4H_9I \rightarrow C_4H_8 + HI, \quad (2)$$

$$MgO + 2HI \rightarrow MgI_2 + H_2O. \quad (3)$$

According to the thermodynamic calculations [10], the equilibrium of reaction (2) should be shifted to the left up to temperatures well above 300 °C, and the HCl abstraction should occur much more easily. This can be explained by the fact that the energy gain due to the HI abstraction from C_4H_9I is very small because of a small difference in the energies of C–I and H–I bonds. Meanwhile, reaction (3) is always thermodynamically favorable in the studied temperature range, and it can make the HI abstraction possible even at temperatures below 300 °C. However, this results in the iodination of the MgO surface. After the surface is covered with an iodide layer, subsequent reaction is very difficult because of slow iodine diffusion into the MgO nanocrystals.

Because of the thermodynamic restrictions, reaction (2) should not go by itself at 100 or 200 °C, which is observed experimentally when the 1-iodobutane conversion falls to nearly zero after some time. At 300 °C the thermodynamic limitations are not as strict, which changes the overall picture of the process. Magnesium iodide now starts to act as a dehydroiodination catalyst, providing stable conversion of 1-iodobutane to butenes.

3.4. Adsorption measurements

Adsorption-desorption isotherms for initial AP-MgO and for samples 3 and 6 are presented in the bottom part of Fig. 7 in regular coordinates. The top part presents the linear parts of corresponding comparative plots. These isotherms appear to be typical for AP-MgO and its derivatives [11,19]. As discussed elsewhere [11,19], the texture of these materials can be described as a unity of mesoporous aggregates of nonporous solid particles several nanometers in size.

Changes in the specific surface areas of MgO after reaction with 1-iodobutane at different temperatures are presented in Table 1. Initial AP-MgO is referred to as sample 1. The samples after reaction with 1-iodobutane at 100, 200, 300, 350, and 400 °C are referred to as 2–6, respectively. Sample 7 is the sample treated at 500 °C in an argon flow after reaction with 1-iodobutane at 200 °C.

As the reaction temperature increases, the specific surface area of the samples calculated by the BET method gradually decreases from 410 m^2/g (starting AP-MgO) to 97 m^2/g (after reaction at 400 °C). The surface area measured by the comparative plot method also decreases from 430 to 90 m^2/g. As reported above, the weight of the samples also changes during the reaction (Fig. 1). The ultimate increase in sample mass related to the initial sample mass, X, is reported in Table 1.

To follow the change in geometrical surface area one has to take into account the weight changes. The surface areas

Table 1
Textural characteristics of AP-MgO samples after reaction with 1-iodobutane at different temperatures

Sample	X[a] (g/g)	S.A.$_{BET}$[b]		S.A.$_{comp}$[c] (m^2/g)		Intercept on comparative plot (mL/g)	V[c] (cm^3/g)	"Guest" (species/nm^2)
		m^2/g of sample	m^2/g of initial MgO	m^2/g of sample	m^2/g of initial MgO			
1	0	409	409	427	427	−0.010	0.94	–
2	0.145	342	400	354	414	−0.025	0.74	2.0
3	0.184	240	294	278	341	−0.020	0.62	3.7
4	0.115	178	201	227	257	−0.018	0.65	3.1
5	0.083	146	159	193	211	−0.019	0.84	2.7
6	0.039	97	101	121	126	−0.010	0.57	1.9
7	0	90	90	106	106	−0.007	0.54	–

[a] Amount of "guest" component, g of "guest" component per g of material after reaction.
[b] Surface areas.
[c] Mesopore volume.

normalized to the weight of the initial AP-MgO are also reported in Table 1. No change in geometrical surface area of AP-MgO can be seen until the reaction temperature reaches 200 °C. At higher temperatures a significant drop in the geometrical surface is observed.

These data correlate well with the results of our previous studies of the 1-chlorobutane reaction with AP-MgO [11]. However, there is also a significant difference in the textural behavior of AP-MgO in these two cases. In the case of 1-chlorobutane almost all pores are filled with $MgCl_2$ phase at temperatures above 300 °C. Reaction with 1-iodobutane is accompanied by a decrease in the pore volume of less than twofold (Table 1). Taking into account a small change in the sample weight during this reaction, there is no doubt that bulk MgI_2 is not formed. The drop in the surface area and pore volume appears to result from the sintering of the nanoparticles in the presence of halogenated compounds.

This sintering occurs also when the reaction is stopped, but AP-MgO is still treated at elevated temperatures. For example, sample 2 after reaction at 200 °C was subjected to treatment at 500 °C in the argon flow (sample 7). The decrease in surface area and pore volume was even higher than for sample 6, which was treated only in the reaction with 1-iodobutane. We can conclude here that sintering occurs in the presence of surface iodine-containing species rather than because of reaction conditions in the gas phase.

Because of the high atomic weight of iodine, one can make an estimation of the number of "guest" surface iodine species per square nanometer (Table 1), assuming their molecular weight to be equal to that of iodine atom. The number of "guest" surface species proved to be in the range of 2–4 species/nm^2 for all samples after reaction. Such low concentration of the "guest" molecules allows us to assume that they are molecularly dispersed on the surface. The highest concentration of "guest" species was found for sample 3 after reaction with 1-iodobutane at 200 °C, which shows maximum weight gain as well. The surface concentration of the iodine-containing species decreases as the reaction temperature increases.

Another confirmation of this conclusion comes from comparative plots (Fig. 7). These plots are linear but have negative intercepts that increase in absolute value with increasing concentration of "guest" surface species (Table 1). As discussed earlier [19], the most probable origin of the negative intercepts on comparative plots is the presence of molecularly dispersed modifiers. This is most likely the exact case for AP-MgO treated with 1-iodobutane.

4. XPS, XFSA, and elemental analysis data

As mentioned above, the XRD study of MgO samples after reaction with 1-iodobutane did not reveal the presence of the MgI_2 phase. Nevertheless, the results of the adsorption experiments and analysis of reaction products indicate that the MgO surface is subjected to significant chemical modification. To analyze the causes of the MgO weight gain during reaction with 1-iodobutane, we used additional physicochemical methods (XPS, XFSA, and elemental analysis). The results of such analysis for AP-MgO samples treated with 1-iodobutane at 100 and 300 °C are reported in Table 2.

XPS spectra in the I $3d_{5/2}$ region are presented in Fig. 8. The spectra clearly show that no significant changes occur in the state of iodine when the reaction temperature is increased from 100 to 400 °C. Most of the iodine corresponds to the ionic state I^- in magnesium iodide [20,21]. Weak additional lines appear at higher bonding energies of 624–627 eV. They most likely correspond to iodine chemically bound with carbonaceous residues. The amount of iodine in these states does not exceed 1% of the total amount of iodine in the samples.

The total number of iodine atoms relative to the number of magnesium atoms is low, only about 2.9% (see Table 2). Therefore, no shoulders corresponding to Mg^{2+} ions in MgI_2 are observed in the Mg 2s spectra. As the MgI_2 phase is not detected by XRD, it is natural to assume that I^- observed in the samples corresponds to a surface iodide.

It is important to understand that the iodine concentration in the surface monolayer must be much higher than 3%.

Table 2
Results of XPS, XFSA and elemental analysis of AP-MgO after reaction with 1-iodobutane at 100 and 300 °C

T (°C)	$\Delta P/P_0$	$\Delta P/(P_0+\Delta P)$	Elemental analysis data (wt%)			XFSA data I (wt%)	XPS data[a] I (at%)
			I	C	(I + C)		
100	15.3	13.4	8.9	4.4	13.3	8.9	3.0
300	13.4	11.8	9.1	1.7	10.8	7.3	2.7

[a] The depth of the surface layer is about 30 Å.

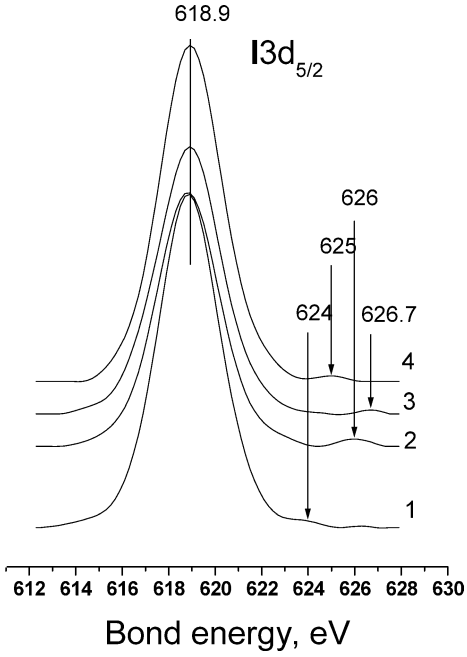

Fig. 8. XPS spectra of I $3d_{5/2}$ region of AP-MgO samples after reaction with 1-iodobutane at different temperatures: 1—100; 2—200; 3—300; and 4—400 °C.

The electron emission from the samples was performed with a mild Al-K_α X-ray irradiation. So the average free path of electrons λ was between 20 and 30 Å, depending on the line in the spectrum. For the Mg 2s region it was equal to 30 Å. The lattice parameter in the face-centered cubic lattice of MgO is 4.21 Å, so that the minimum distance between Mg atoms is 2.105 Å. This means that the depth of the surface layer studied by XPS is about 15 monolayers. Thus, assuming that all iodine is located in one surface monolayer, the iodine concentration in this monolayer can be estimated to be 45 at%. In other words, a significant part of the MgO surface is covered with iodine after reaction.

The elemental analysis showed that the MgO samples after reaction with 1-iodobutane contain carbon and iodine (Table 2). The combined contents of I and C agree well with the weight gain observed in the gravimetric experiments. Note that the concentration of carbon on the MgO surface is 2.5 times higher after reaction at 100 °C in comparison with the reaction at 300 °C. Meanwhile, the iodine contents in the two cases are similar (about 9 wt%). The iodine contents calculated from the XFSA results agree very well with the elemental analysis data (Table 2).

5. Conclusion

Thus, there is no bulk MgI_2 formation during the reaction of 1-iodobutane with AP-MgO. However, the modification of surface by I^- leads to a change in reaction selectivity. The iodinated surface begins to act as a Lewis acid by a stage E1 mechanism of iodine elimination from 1-iodobutane. The iodination also resulted in 2-iodobutane formation by reversible reaction of HI with butene over iodinated surface of magnesium oxide.

Acknowledgments

The financial support of the U.S. Army Research office, CRDF (Project RC1-2340-NO-02), and Russian Department of Industry and Science (Project SS-2120.2003.3) is acknowledged with gratitude.

References

[1] Y.-X. Li, K.J. Klabunde, Langmuir 7 (1991) 1388.
[2] Y.-X. Li, O.B. Koper, M. Atteya, K.J. Klabunde, Chem. Mater. 4 (1992) 323.
[3] O.B. Koper, J. Lagadic, A.M. Volodin, K.J. Klabunde, Chem. Mater. 9 (1997) 2468.
[4] O.B. Koper, J. Lagadic, K.J. Klabunde, Chem. Mater. 9 (1997) 838.
[5] O.B. Koper, K.J. Klabunde, Chem. Mater. 9 (1997) 2481.
[6] O.B. Koper, Y.-X. Li, K.J. Klabunde, Chem. Mater. 5 (1993) 500.
[7] K.J. Klabunde, J.V. Stark, O.B. Koper, C. Mohs, D.G. Park, S. Decker, Y. Jiang, J. Lagadic, D. Zhang, J. Phys. Chem. 100 (1996) 12142.
[8] Y. Jiang, S. Decker, C. Mohs, K.J. Klabunde, J. Catal. 180 (1998) 24.
[9] H. Itoh, S. Utamapanya, J.V. Stark, K.J. Klabunde, J.R. Schlup, Chem. Mater. 5 (1993) 71.
[10] I.V. Mishakov, A.F. Bedilo, R.M. Richards, V.V. Chesnokov, A.M. Volodin, V.I. Zaikovskii, R.A. Buyanov, K.J. Klabunde, J. Catal. 206 (2002) 40.
[11] V.B. Fenelonov, M.S. Mel'gunov, I.V. Mishakov, R.M. Richards, V.V. Chesnokov, A.M. Volodin, K.J. Klabunde, J. Phys. Chem. B 105 (2001) 3937.
[12] V.V. Chesnokov, A.F. Bedilo, D.S. Heroux, I.V. Mishakov, K.J. Klabunde, J. Catal. 218 (2003) 438.
[13] R. King, Process Engineering March (1977) 85.
[14] S. Utamapanya, K.J. Klabunde, J.R. Schlup, Chem. Mater. 3 (1991) 175.
[15] C.L. Carnes, P.N. Kapoor, K.J. Klabunde, J. Bonevich, Chem. Mater. 14 (2002) 2922.
[16] A.P. Karnaukhov, V.B. Fenelonov, V.Yu. Gavrilov, Pure Appl. Chem. 61 (1989) 1913.
[17] V.B. Fenelonov, V.N. Romannikov, A.Yu. Derevyankin, Micropor. Mesopor. Mater. 28 (1999) 57.

[18] S.J. Gregg, K.S.W. Sing, Adsorption, Surface Area and Porosimetry, Academic Press, London, 1982.

[19] M.S. Mel'gunov, E.A. Fenelonov, V.B. Mel'gunova, A.F. Bedilo, K.J. Klabunde, J. Phys. Chem. B 107 (2003) 2427.

[20] J.F. Moulder, W.F. Stickle, P.E. Sobol, K.D. Bomben, Handbook of X-Ray Photoelectron Spectroscopy, Perkin–Elmer, Eden Prairie, MN, 1992.

[21] D. Briggs, M.P. Seah, Practical Surface Analysis: By Auger and X-Ray Photo-Electron Spectroscopy, Wiley, New York, 1983.

[22] J.V. Stark, D.G. Park, J. Lagadic, K.J. Klabunde, Chem. Mater. 8 (1996) 1904.

[23] S. Decker, K.J. Klabunde, J. Am. Chem. Soc. 118 (1996) 12465.

[24] H. Noller, P. Andreu, M. Hunger, Angew Chem. Internat. Edit. 10 (1971) 172.

[25] H. Knozinger, H. Buhl, Z. Phys. Chem. 63 (1969) 199.